ELSEVIER

Journal of Structural Geology 28 (2006) 1114–1122

JOURNAL OF STRUCTURAL GEOLOGY

www.elsevier.com/locate/jsg

Isotopic indicators of deformation in the Red Sea

Claudio Vita-Finzi *, Baruch Spiro

Natural History Museum, Cromwell Road, London SW7 5BD, UK

Abstract

Palaeostress analysis of spreading oceanic ridges requires data on extension over time and at different locations along strike so that mechanical models can be formulated and tested. The seafloor palaeomagnetic record provides average spreading rates but as the last (normal) chron measures 790,000 years an alternative method is required for identifying episodes of spreading at time scales of $<10^3$ yr which can be fused with seismic and geodetic sequences. On the assumption that the level of hydrothermal circulation on the sea floor is linked with tectonic activity, palaeotemperature and geochemical changes in the seawater determined from cores of the sea floor sediments should serve as proxies for episodes of extension provided they can be dated and alternative explanations for them ruled out. The Red Sea provides a study area for evaluating this proposal because it is a marginal sea with a shallow threshold which limits mixing with the open ocean especially during periods of low sea level, it receives little runoff from the arid lands that surround it, and its median ridge is hydrothermally active. Chemical evidence has been reported for two broadly synchronous late Quaternary hydrothermal episodes in the Atlantis II and Thetis deeps; $^{87}Sr/^{86}Sr$ ratios in the Atlantis II deep are thought to reflect variations in hydrothermal activity. Published $\delta^{13}C$ and $\delta^{18}O$ data from cores both within brine pools and outside them indicate fluctuations during the Holocene for which no climatic counterparts on bordering land areas or in the Arabian Sea are documented; moreover our study has revealed a major (positive) $\delta^{18}O$ excursion older than 40,000 yr in *Globigerinoides ruber* in Core CH10003-3 PC at a depth of 1374 m which is not associated with hardgrounds or a $\delta^{13}C$ fluctuation and which may have resulted from a hydrothermal pulse. There is no such signal in the core for events of magnitude up to 8.3 that are recorded in the palaeoseismic record of the last 50,000 yr in the Lisan Marls, which suggests that the $\delta^{18}O$ pulse from Core CH10003-3 corresponded with an event of $M>8.3$ in the RedSea-Dead Sea rift system Other isotopes may prove to be more sensitive and therefore responsive to smaller deformation.

Keywords: Hydrothermal; Extension; Palaeomagnetic; Red Sea; Isotopes

1. Introduction

Much of current palaeostress analysis of ocean spreading centres hinges on earthquake data and the motivation is indeed often to understand Seismic risk. Modern regional tectonic analysis focuses on plates whose boundaries and kinematics are defined primarily by hypocentre distribution. Sequences of brittle strain events are commonly grouped together into stress regimes or stages. For instance, the late Neogene deformation of central and eastern Crete can be subdivided into three episodes of basin extension following a period of approximately N–S compression (Ten Veen and Postma, 1999) and Permian–Cenozoic deformation of central and northern England and Wales falls into five tectonic stages (Hibsch et al., 1995). But, as Plenefisch and Bonjer (1997) observe, even if microtectonic analyses are highly successful in determining the orientation and relative age of superimposed palaeostress fields, they can rarely supply absolute ages for the various deformation phases. The problems of interpretation are compounded when the structure under review is submarine, as reliance now has to be placed almost wholly on focal-plane solutions, and strain analysis is accordingly confined to the last few decades.

The present paper is an attempt to contribute to deformation analysis in this kind of setting by exploring the potential of isotope geochemistry for identifying episodes of enhanced tectonic extension and shear. The discussion is based on the Red Sea, a juvenile ocean whose evolution for the last ~30 Myr has been inferred largely from the geomagnetic reversals recorded on its floor. Our central thesis is that major episodes of seafloor spreading in the Red Sea system will be reflected in pulses of hydrothermal activity at the ridge and consequently in the local seawater and associated sedimentary deposits and by changes in the local microfaunal assemblages in response to local environmental (water chemistry and temperature) conditions (Vita-Finzi, 2001). Hydrothermal systems may respond to levels of earthquake activity more

* Corresponding author. Fax: +44 20 77944415.
E-mail address: cvitafinzi@aol.com (C. Vita-Finzi).

0191-8141/$ - see front matter © 2006 Elsevier Ltd. All rights reserved.
doi:10.1016/j.jsg.2006.03.014

than 200 km away and as much as 36 days later (Johnson et al., 2001). Judicious selection of chemical indicators should enable one to distinguish between such tectonic signatures and the products of climatic and related sea-level and depositional episodes. For this notion to be valid it is not necessary to assume that bottom waters in the Red Sea are connate, as did Brewer et al. (1965), because seawater circulates through ocean ridges and in so doing acquires heat and chemicals (Bach and Humphris, 1999).

Location in a marginal sea should bring analytical benefits as well as disadvantages: the contribution of local hydrothermal sources to water chemistry is enhanced by relative isolation from the world ocean. Of course, changes in temperature and salinity arising from global sea-level fluctuations are also enhanced, but some check on them can come from comparative isotopic determinations immediately outside the mouth of the Red Sea and from the neotectonic history of the Red Sea and adjoining land areas.

2. Tectonic setting and background

The Red Sea separates the Arabian plate from the Nubian portion of the African plate (Fig. 1). It is widely seen as the archetypal extensional ocean basin in its initial stages. At its northern end it branches into the Gulf of Suez and the Gulf of Aqaba. The line of separation between the African and Arabian plates is well defined by seismicity (Fig. 2) north of about 17°30′N. South of this latitude, a second seismic boundary

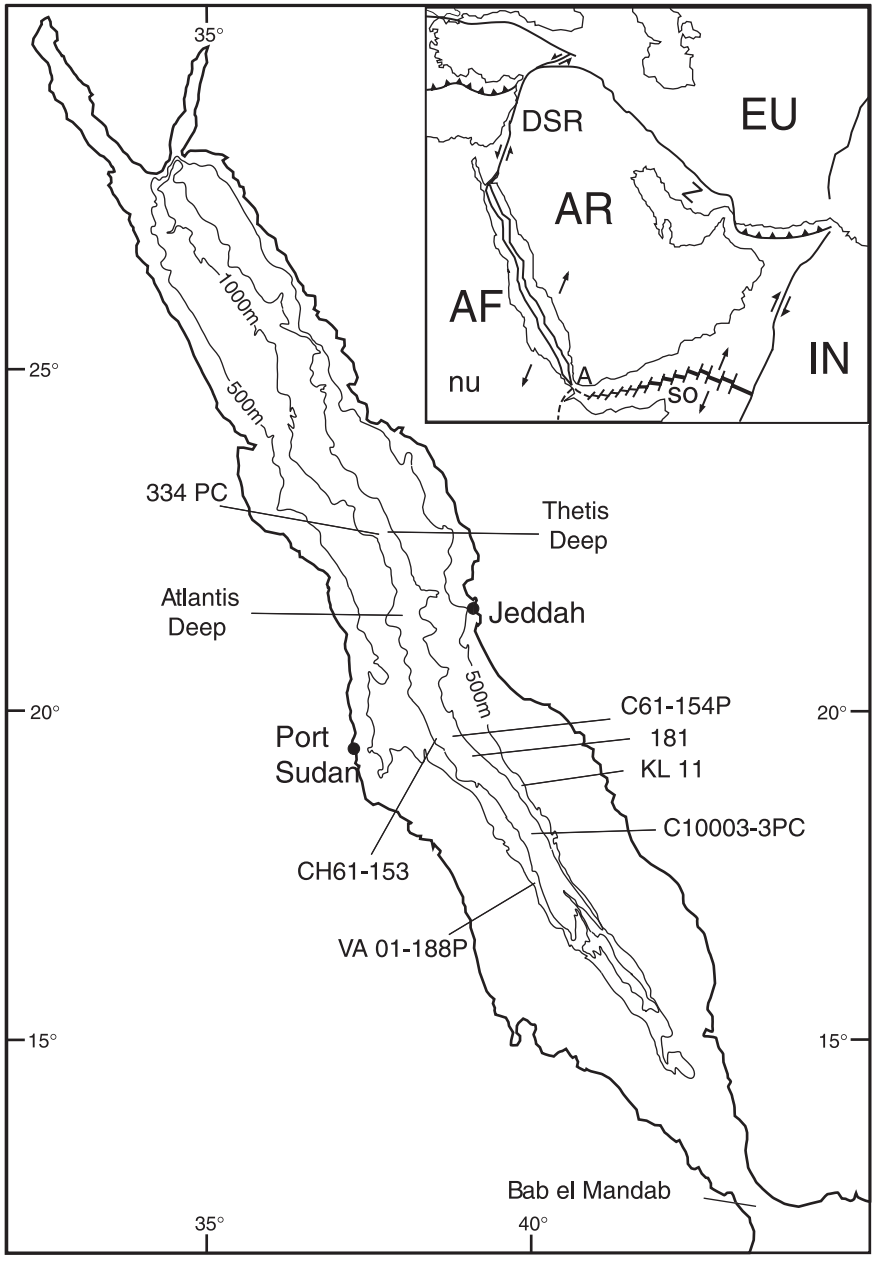

Fig. 1. Location of study area showing cores and deeps mentioned in text. Inset shows plate-tectonic setting. Z = Zagros, DSR = Dead Sea rift. The line of separation between the Nubian (nu) and Somalian (so) sub-plates meets the Red Sea rift at the Afar (A) triple junction.

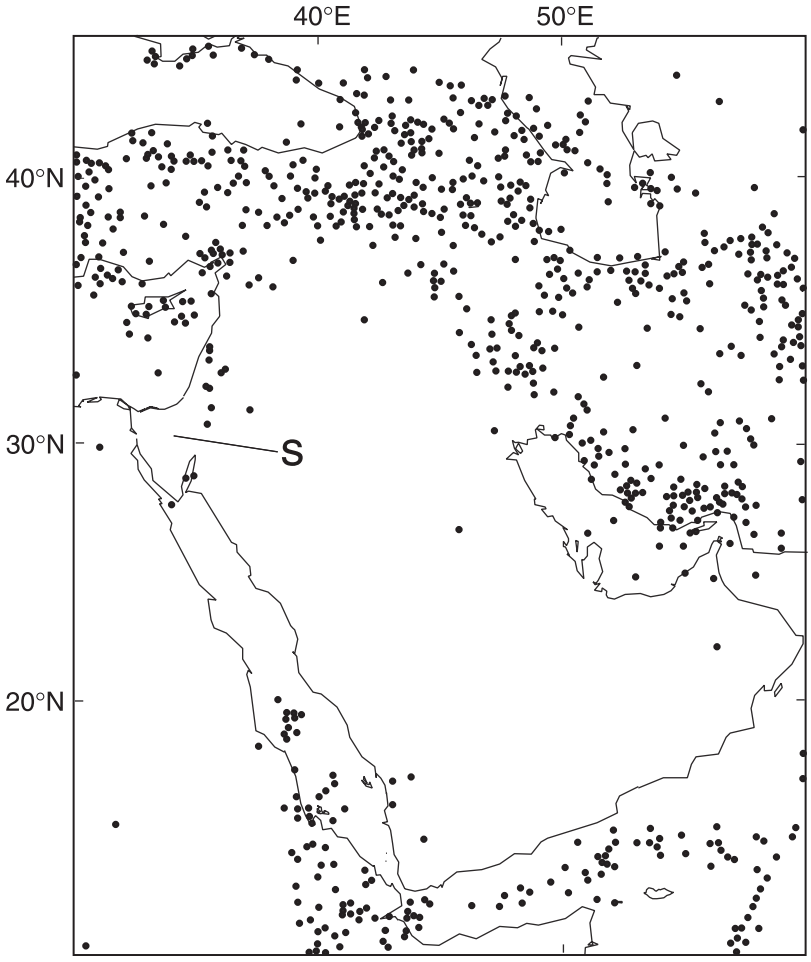

Fig. 2. Regional seismicity (M≧5.0, AD 10-1999), courtesy of NDGC/NOAA. s=Sinai block.

branches off to the SW to define what Chu and Gordon (1998) call the Danakil microplate. The evolution of the Red Sea thus bears on the geodynamics of East Africa and the Levant as a whole, not to mention oceanic history in general.

There are two major schools of thought about the early history of the Red Sea. The classic work by Girdler and Styles (1974) postulated a two-stage history of spreading, the first lasting from 41 to 34 Myr ago and the second dating from the last 4–5 Myr. Some workers find evidence for simultaneous opening along its entire length (e.g. Omar and Steckler, 1995), whereas others favour progressive rifting (e.g. Bonatti, 1985). Most workers agree, however, that the late stage in the sea's evolution has been characterised by south-to-north propagation. Spreading rates spanning the last 3–4 Myr are provided by the palaeomagnetic record of the seafloor. Only an average rate can be secured for the last (normal) subdivision of this sequence spanning 790,000 years (Shackleton et al., 1990), but, using 64 rates for the last 3.2 Myr for all the magnetic profiles between 15°54′ to 26°N, Chu and Gordon (1998) were able to show that the fastest spreading rate of ∼16 mm/yr applies near 18°N and the slowest of 10 mm/yr at 25°30′N. As regards separation between Sinai and Africa, Bosworth and Taviani (1996) calculated a Late Pleistocene rate of 0.8–1.2 mm/yr. GPS determinations by McClusky et al. (2003) are consistent at the 95% confidence level with the Nubia–Arabia Euler vector (31.5±1.2°N, 23.0±2.7°E, 0.40±0.05° Myr^{-1}) obtained by Chu and Gordon (1998).

In a paper endorsing Bonatti's (1985) punctiform model for the Red Sea, Makris et al. (1991) showed that microearthquakes with maximum hypocentre depths of 18 km are concentrated along the margins of the axial trough and grabens within it, with the eastern graben margins more active than the western. Earthquakes with focal depths of <1000 m were found to cluster in the centre and east of the deep trough in association with hydrothermal circulation, and thus confirmed that the locus of enhanced extension will favour both the penetration of sea water and the release of heated waters.

The instrumental record includes only one measured hydrothermal anomaly within the Red Sea, during which two substantial earthquakes occurred within the Rift but no local deformation was reported. The anomaly amounted to a modest rise in temperature from 55.9 to 67.2 °C which was recorded in the Atlantis II deep (21°21′N, 38°04′E) between 1965 and 1997 and which was ascribed to increased hydrothermal activity (Hartmann et al., 1998). The earthquakes were one of $M_s>6.0$ (1977.12.28, 16.54°N, 40.29°E) within the Red Sea but about 500 km SE of the deep (Ambraseys, 2001), and the Nuweiba earthquake of 1995.11.22 ($M_w=7.2$), the largest seismic event

along the Dead Sea Transform of the last 160 yr, which ruptured 45–50 km along the strike-slip fault system occupying the Gulf of Aqaba (Shamir et al., 1993; R. Amit, pers. comm.), 900 km NW of the deep. Neotectonic chronologies at the Arabian plate margins (Vita-Finzi, 2001) suggest that major pulses of slip at the Red Sea are diffusely distributed across the plate and are manifested as shear on the Dead Sea rift as well as compression at the Zagros (z in Fig. 1, inset). In effect, seismically-generated deformation at the ridge accounts for the bulk of Arabian plate translation, analogous to the situation described by Wernicke et al. (2000).

3. Chemical indicators of palaeostress

One way forward is to find chemical proxy records of enhanced hydrothermal circulation for which a tectonic explanation is plausible. Despite their stagnant nature, some of the deeps offer certain advantages for such an enterprise. Pierret et al. (2001) had concluded that the variety of processes responsible for brine formation would create differences in hydrothermal activity along the Red Sea axis. Yet differences in the timing of activity in the various deeps are to be expected by virtue of the segmented nature of the constituent faults. Scholten et al. (1991) found evidence for intermittent brine filling in the NE Thetis Deep (Fig. 1) in the form of Fe/Mn partition, as a low Eh in a stable brine pool keeps the Mn in solution so that it can diffuse out whereas the Fe remains in the

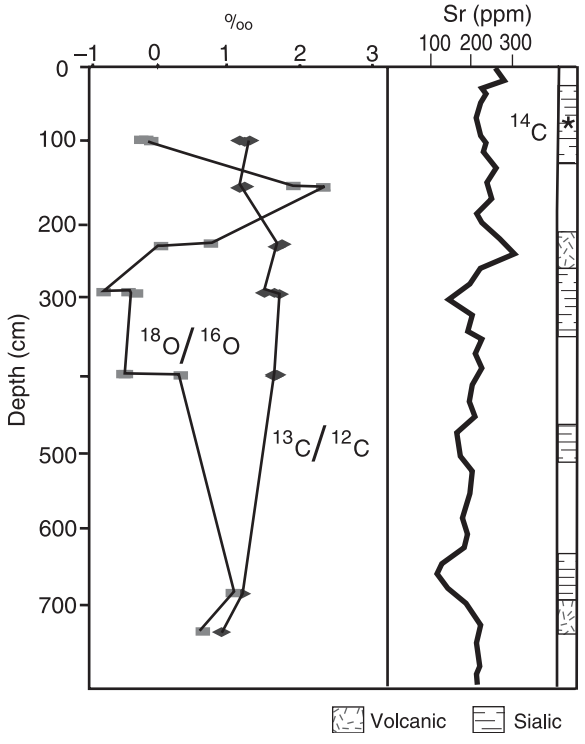

Fig. 3. Data for *Globigerinoides ruber* from Core CH10003-3PC. (Left) $\delta^{13}C$ and $\delta^{18}O$ rel. VPDB (‰, mean of three determinations); (right) Sr concentration in non-carbonate fraction (ppm) and lithological units after Boger and Faure (1974).

basin. Using ^{14}C ages on calcareous fossil layers in an analysis of one of two sea floor cores (334PC), they identified an episode of hydrothermal activity dating from 23,000 to 14,000 yr BP, which was at a maximum during the first 3000 yr, and a second peak at 10,000–1200 yr BP, with a maximum during 2700–1200 yr BP. Scholten et al. (1991) drew attention to similar episodes in the Atlantis II deep, at a distance of 160 km, during 20,000–17,000 yr BP and $<$10,000 yr BP (Ku et al., 1969). Although we defer comparison with tectonic events on land, it is instructive to note that the Lisan Marl chronology includes an event dated to 24.4 kyr (Marco et al., 1996). There is, however, a regrettable gap in the seismic record between the end of Lisan deposition $\sim$18,000 yr BP and the historical period.

A second potential indicator of enhanced hydrothermal activity is the $^{87}Sr/^{86}Sr$ ratio in bottom waters. Blanc et al. (1995) found that the water of the Atlantis II deep was a mixture of palaeowaters, interstitial waters and hydrothermal inputs, so that the hydrothermal inputs could not be evaluated using oxygen, hydrogen and strontium isotopes separately. Yet the $^{87}Sr/^{86}Sr$ ratio in fossil marine carbonate could lead to an estimate of the relative contributions of seawater and hydrothermal fluids (Spooner et al., 1977). Analysis of this ratio in two cores from the Atlantis II deep by Anschutz et al. (1995) suggests that, once the brine pool had been established (their Unit 1 in Core 684), it remained isolated from seawater so that mineralogical changes reflected variations in the temperature and flow rate of hydrothermal fluids into the deep.

The effect was not confined to the deeps and Starinsky et al. (2002) have suggested that lower $^{87}Sr/^{86}Sr$ ratios in planktonic foraminifera from the Red Sea relative to the Gulf of Aden reflect a greater role for hydrothermal (as opposed to 'erosional') sources of strontium during periods of low sea level. The $^{87}Sr/^{86}Sr$ ratio had previously been used by Boger and Faure (1974, 1976) and Boger et al. (1980) to identify the source of the non-carbonate fraction in Red Sea sediments recovered from piston cores and more specifically to distinguish between the weathering products of rocks from Arabia and material derived from young volcanics. The former were likely to have Sr concentrations $<$200 ppm and $^{87}Sr/^{86}Sr$ ratios generally between 0.710 and 0.720. The corresponding values for recent volcanics, based on Holocene material from Red Sea islands, were 774 ppm and $\sim$0.704. On the basis of a hyperbolic mixing curve they calculated the contribution of the two putative Sr sources in core 10003-3PC, taken on a Woods Hole R.V. Chain cruise from the median valley of the southern Red Sea at a depth of 1315 m. The core displays an alternation of what they termed volcanic and sialic deposits. The results are shown in the right hand curve of Fig. 3. In their view, the volcanogenic component has contributed 20–25% of the non-carbonate fraction, with a progressive increase up the core and two distinct episodes of increased volcanogenic deposition. Increases in sialic deposition (Fig. 3) were also noted and tentatively ascribed to climatic changes. In short, if these two sources can be held

constant it may be possible to evaluate the strontium contributed by hydrothermal sources.

This paper points to a third potential guide to hydrothermal fluctuations in the record, that provided by the stable isotopes $\delta^{13}C$ and $\delta^{18}O$. They are, of course, conventionally viewed as indicators of climatic and related sea level changes. For example, in an analysis of glacioeustatic control of salinity in the last 20,000 yr, which was based on oxygen isotopes for *Globigerinoides ruber* and calibrated with two ^{14}C dates, Thunell et al. (1988) showed that glacial–interglacial contrasts had a greater amplitude in the Red Sea (core CH61-153, −2704 m) than in the Gulf of Aden (core RC9-166, −739 m). Their $\delta^{18}O$ data for the former, which they emphasised was not in a brine pool, displayed at least nine marked negative oscillations during the last 20,000 yr. Almogi-Labin et al. (1991) likewise analysed the $\delta^{18}O$ of pteropods from cores KL11 (−825 m) and Station 181 (−166 m). *Creseis acicula*, which of the species analysed provided the most complete isotopic record, showed little change in its $\delta^{18}O$ over the last 13,000 yr (the chronology was based on correlation with postglacial $\delta^{18}O$ curves in the Red Sea and outside it) but its $\delta^{13}C$ indicated five oscillations between ~13,000 and ~4600 yr BP. Frequencies of this order are reported for climatic data for various parts of the world, but neither sea-level oscillations nor fluvial inputs that could account for these oscillations have yet been reported for the Red Sea catchment.

Core KL11 also played a key role in the work by Siddall et al. (2003, 2004) on deriving global sea level (and thence ice volumes) from the $\delta^{18}O$ of the Red Sea for the last 470,000 yr, although analytical uncertainty limited the reconstruction to sea-level oscillations of 12 m or more. Diagenetic alteration of the foraminiferal calcite by hot brines was avoided by focusing on records from relatively shallow (<1000 m) locations away from the axial trough of the Red Sea. The results for the period 70,000–25,000 yr based on *G. ruber* showed a striking resemblance to the Byrd and Vostok ice-core climatic records in its general trend.

The palaeoclimatic interpretation of stable isotopes derived from Red Sea cores taken in the median valley is perhaps best illustrated by the classic study by Deuser and Degens (1969), which yielded pronounced oscillations in both $\delta^{18}O$ and $\delta^{13}C$ from pteropods and foraminifers and which underpinned their interpretation by ^{14}C dating and geochemical analyses of the host sediments. In core CH61-154P, for example, the $\delta^{18}O$ of planktonic foraminifers attained +3‰ at least twice during the last glacial, the last time represented by material from a depth of 225–250 cm, and that of pteropods attained and even exceeded +6‰ during the same period. These peaks were associated with lithification of the sediments and encrustation of the fossils by aragonite. There are corresponding increases in $\delta^{13}C$ but they are far less pronounced. The fluctuations were taken to reflect periods of lowered sea level, which restricted the exchange of water between the Red Sea and the Indian Ocean, although Deuser and Degens (1969) also raised the possibility that the controlling factor was tectonic activity near the Bab el Mandab.

4. Sampling strategy and results

In order to explore the hydrothermal model we carried out a pilot study combining Sr isotopes with $\delta^{13}C$ and $\delta^{18}O$. The material came from the core (to which they refer as 100-3-3p) investigated by Boger and Faure (1974) and mentioned earlier. The first step was to discover whether the oscillations in strontium reported by them on the non-carbonate fraction from this core (Fig. 3) were echoed in the $^{87}Sr/^{86}Sr$ ratios in foraminiferal carbonate. This would indicate a relationship between the Sr dissolved in sea water and the lithologies deposited at the same time and thus help to distinguish between hydrothermal and detrital sources. Sampling followed the lithological division of the core by Boger and Faure (1974) into normal, sialic and volcanic sections. The top 30 cm were cemented and the microfauna could not be separated; some cement was also present at 70 cm. Lithified layers were reported from earlier Chain cruises in the central Red Sea by Deuser and Degens (1969); the uppermost consisted of aragonite, whereas lower layers were composed primarily of magnesian calcite, which Milliman et al. (1969) interpreted as the product of inversion from aragonite.

The remaining samples in our core were rich in microfauna, although they differed considerably in the relative abundance

Table 1
$^{87}Sr/^{86}Sr$ data for core CH10003-003PC

depth (cm)	unit+	sediment type[x]	$^{87}Sr/^{86}Sr$ non-carbonate fraction[+]	$^{87}Sr/^{86}Sr$ *G. ruber*[x]
90	2	sialic	0.70664	
94				0.709198
95				0.709203
96				0.709196
155	3	normal		0.709196
170			0.70639	
220			0.70605	
240	4	volcanic	0.70556	
296	5	sialic		0.709204
302			0.70901	
404	6	normal		0.709195
430			0.70700	
450			0.70699	
470	7	sialic	0.70831	
520	8	normal	0.70686	
600			0.70718	
620			0.70695	
652	9	sialic	0.70998	
670			0.70900	
690	10	volcanic	0.70708	
740			0.70701	
742				0.709234
782		?	0.70689	

+ after Boger and Faure, 1976
x after Viger and Faure, 1974
* this study

of Foraminifera and other microfauna and the local occurrence of moulds of pteropods and of mica flakes. The 'normal' sediments at 154–155 cm were marked by a scarcity of foraminifers and an abundance of moulds and mica, whereas the 403–406 cm material contained only microfauna in this fraction. The 'sial' samples were marked by an abundance of microfauna and the absence of moulds of pteropods and mica. The 'volcanic' deposits yielded few microfauna, some mica and, locally, a few moulds.

Tests of *G. ruber* were selected for dating from samples at 60 and 80 cm. In addition, where possible three consecutive samples 1 cm in thickness were taken at depths of 155–158 and 403–406 cm to represent 'normal' sediment, 94–97 and 295–298 cm to represent 'sial' and 232–235, 692–694 and 742–743 cm to represent volcanic rocks. Well preserved and clean tests of *G. ruber* from these samples were picked for $\delta^{13}C$ and $\delta^{18}O$ analysis and for seven $^{87}Sr/^{86}Sr$ determinations (see Appendix A). Samples 1 cm thick were also taken at intervals of 10 cm from the top 1 m defined as 'normal' by Boger and Faure (1974). The state of preservation of the pteropods (and other aragonitic shells) was attributed by Almogi-Labin et al. (1986) to variations in the initial concentration of organic matter in the sediment.

As shown in Table 1 and Fig. 3, there is little variation in the planktonic $^{87}Sr/^{86}Sr$ for a depth range with substantial diversity in the Sr content and $^{87}Sr/^{86}Sr$ ratios of the corresponding non-carbonate fraction of the sediment, confirmation that the detrital Sr reservoir may not have a significant effect on the dissolved Sr available to the calcareous plankton. This conclusion does not preclude further attempts to use Sr as palaeostress indicator, for instance within one of the deeps, but merely eliminates it from the present discussion. The $\delta^{13}C$ data, though somewhat more variable, for the most part fluctuate by less than $\pm 0.5‰$ and there is no evidence that they are allied to the Sr sequence. In contrast, the $\delta^{18}O$ curve displays substantial variations that are independent of the others and of which the latest, peaking at a depth of 150 cm (within the 'normal' lithology of Boger and Faure (1974)) amounts to almost 2.5‰. The peak is $>4.0‰$ more positive than the average of $-2.24‰$ ($n=15$) reported by Auras-Schudnagies et al. (1989) for *G. ruber* from surface waters and core tops in the southern Red Sea.

The timing of the $\delta^{18}O$ spike remains uncertain. Boger and Faure (1976) had obtained two ^{14}C ages for the core, one of $21{,}150 \pm 1000$ yr at a depth of 75–85 cm and another of $>32{,}000$ yr at a depth of 185–195 cm. In an attempt to refine the chronology we submitted a sample of *G. ruber* from a depth of 96–97 cm for AMS ^{14}C dating and obtained an uncorrected date of $40{,}430 \pm 900$ yr ($\delta^{13}C = 0.9‰$) (BETA-187497). As this is near the limit of the method the result must be treated as provisional, even though there is no evidence of contamination by younger or older carbon, but it confirms that sedimentation rates at the core site were low.

5. Discussion

Following Schoell and Risch (1976), and Milliman et al. (1969) before them, we provisionally equate the core-top and the 70 cm cemented horizons with a time of lowered sea level, which is widely thought to have reached its peak ~19,000 yr ago. The finite ^{14}C date of $21{,}150 \pm 1000$ yr is consistent with this proposal. The absence of an ^{18}O peak in the uppermost part of the core, like the absence of aragonitic cementation and of a $\delta^{13}C$ anomaly, argue against an explanation for the $\delta^{18}O$ spike at ~150 cm in terms of salinity and lowered sea level. Indeed the argument can be extended to Core 154, where only one of the stable isotope peaks corresponds with a phase of aragonitic cementation. The sawtooth shape of the ^{18}O curve reported by Deuser and Degens (1969) is reminiscent of other palaeoclimatic indicators where gradual onset is followed by rapid decay, but it can be explained by the close of hydrothermal activity just as well as by the sudden resumption of links with the open ocean.

Unaltered basalts from midoceanic ridges have $\delta^{18}O$ compositions in the region of 5.7‰ SMOW (Muehlenbachs and Clayton, 1976), and high-temperature (>350 °C) exchange will enrich percolating seawater in ^{18}O. How fast this occurs is not necessarily a product of spreading rate; indeed, Bach and Humphris (1999) have shown that for O (and Sr) isotopes it is at a maximum at slow oceanic spreading ridges, where fluid conduits are longer and flow is more sustained than at fast spreading ridges. The issue here, however, is not average spreading rate but the incidence of pulses of spreading.

Local GPS data give 2.6 ± 1.1 mm/yr for fault slip on the Dead Sea fault system, but offset features yield values between 3 and 7.5 mm/yr (Allen et al., 2004). These authors observe that it is not necessarily valid to compare GPS-derived slip rates with long-term deformation, but, in the present context, disparities between the two sets of values could reveal episodes of unusual activity or stability. GPS data obtained in 1999 and 2001 indicate northward displacement of Arabia relative to Eurasia at 22 ± 2 mm/yr at $008 \pm 5°$ (Vernant et al., 2004). This is substantially slower than the NUVEL-1A estimate of 30.5 mm/yr at 006° but very similar to the Holocene rate of about 20 mm/yr on an azimuth of 061° obtained from the geometry of Holocene marine terraces on the Iranian shore of the Gulf (Vita-Finzi, 2001). In other words there is prima facie evidence for bodily translation of Arabia consequent on Red Sea spreading and therefore that large events recorded in the Dead Sea Rift are representative of the entire SW margin of Arabia.

The seismic record of the Dead Sea Rift, initially confined to the 4000 yr spanned by the historical period, has now been extended to about 50,000 yr thanks to the identification of seismites in the Lisan marls laid down in the former Dead Sea (Marco et al., 1996) and shown to be characterised by clustering in periods of about 10,000 yr. A columnar section dated by ^{230}Th–^{234}U ages indicated a mean recurrence interval of ~1600 yr for events estimated to be of M_L 5.5. The historical evidence indicates 42 events along the Dead Sea fault system of $6.7 < M_L < 8.3$ in the past 2500 yr, with a recurrence interval in the southern half of the transform of about 1500 yr for $M = 7.3$ (Ben-Menahem, 1991). Fault-slip data along the Dead Sea Transform yield 88 different palaeostress tensors between the Neoproterozoic and the Holocene indicating a

general clockwise rotation with time of the S_{Hmax} axis from an E–W trend in the Cretaceous to a N–S trend in the Pleistocene (Zain Eldeen et al., 2002).

The fact that the level or frequency of seismic activity has not been uniform along the rift is a warning against seeking a single recurrence interval applicable to the entire structure. Granted that the dated seismites provide a full record of large earthquakes at the measured Lisan section, the mean interval between them was 1.63 or 1.49 kyr (according to how the sedimentation rate was measured) but the intervals ranged from 0 to 15.3 kyr and gave standard deviations of 2.86 and 2.26 kyr, respectively. A high-resolution palaeoseismic sequence exposed by the retreating Dead Sea yielded ^{14}C-dated ages which were in good agreement with historical events (barring a period marked by no sedimentation). They indicated the much shorter recurrence interval of ~100–300 yr for $M > 5.5$ events (Ken-Tor et al., 2001).

The AMS ^{14}C age reported here from the Red Sea at 96–97 cm shows that the extensional episode we infer from the δ^{18}O spike is older than 40,000 yr. The preceding period is at least partly covered by the Lisan Marls palaeoseismic evidence of the Jordan Rift, which, it will be recalled, is thought to include events of up to $M = 8.3$. Such events may account for the δ^{18}O oscillations of about 1‰ during the last 20,000 yr in Core CH61-153 (−2704 m) (Thunell et al., 1988; Vita-Finzi, 2001), with its greater resolution and perhaps also by virtue of its greater depth, as well as a minor one at about 10,000 yr BP in Core 154 (Berggren, 1969). From the evidence of Core CH10003-3, one might conclude that the Red Sea has experienced at least one event of $M > 8.3$ in the late Quaternary.

If only earthquakes of this magnitude can accomplish substantial widening of the Red Sea, the process is effectively at an end or at any rate suspended, as suspected by Barberi et al. (1975), and motion has shifted to the African branch of the Afar triple junction. Future work must seek corroboration for the proposed tectonic pattern in other parts of the Red Sea and the coastal record of the Red Sea itself and explore the use of neodymium isotopes: the Nd content of hydrothermal solutions is at least two orders of magnitude higher than that of seawater (Cocherie et al., 1994), its residence time is a mere 300 yr (Faure, 1986), and foraminifers record the Nd isotope composition of the associated sea water and are not affected by the pore fluid in the sediments (Vance et al., 2004). Such a study would also indicate how promptly a hydrothermal change is reflected in the near-surface habitat of the planktonic fauna. Other marginal seas dominated by extension, notably the Gulf of Mexico, and perhaps even less sheltered locations, offer scope for investigating geochemical chronologies of tectonic stress, just as palaeomagnetic analysis of seafloor spreading is now applied to locations lacking the symmetry of the settings where the notion was first formulated.

Acknowledgements

The work discussed here formed part of the Africa–Arabia Connections project led by G. Bailey and supported by the EFCHED programme of the Natural Environment Research Council, UK. We thank the Woods Hole Oceanographic Institution and Ellen Roosen of WHOI for the core samples, Isabel Sanchez Almazo for faunal analyses, Antonio Delgado of CSIC Granada for support with the stable isotope analysis, Ludwig Halicz and colleagues at the MC-ICP-MS Laboratory of the Geological Survey of Israel, Tim Atkinson and Tony Osborn of the Bloomsbury Environmental Isotope Facility for laboratory support as part of a collaborative scheme between University College London, and the Natural History Museum, London and Jody Webster and three anonymous referees for helpful reviews.

Appendix A. Analytical procedure

Samples were prepared for δ^{13}C and δ^{18}O determination according to the method described in Sanchez Almazo et al. (2001). Analyses were carried out on ~0.04 mg aliquots of crushed tests of *G. ruber* at the Stable Isotope Laboratory of the Estación Experimental del Zaidin (CSIC) Granada, using a Finnigan Delta XL mass spectrometer coupled with a Gasbench (both Thermoelectro Corporation). Aliquots of NBS 19 and Carrara Marble were used as running standard. Results are reported relative to VPDB with overall analytical precision at ± 0.1‰ (2 s.d.) for both δ^{13}C and δ^{18}O. Samples were prepared for Sr isotope analysis by acetic acid dissolution followed by ion exchange chromatography using resin Dowex® 50 W–8× 200–400 mesh. Analysis was carried out on a 'Nu Plasma' MC ICP MS (Nu Instruments, Wrexham, UK) at the Geological Survey of Israel. Aliquots of SRM 987 were used as running standard and gave 0.710285 ± 0.00002 (2 s.d.) (see Ehrlich et al., 2001). The quality of the samples for AMS ^{14}C dating was checked by inspection under the binocular microscope and a δ^{13}C determination on an aliquot of the CO_2 prepared for conversion to graphite. Comparison with the δ^{13}C measurements on modern surface waters in the southern Red Sea (Naqvi and Fairbanks, 1996) thus led to rejection of an AMS ^{14}C date for a horizon at −94–95 cm in Core 10003-3PC because its negative δ^{13}C (−1.4‰) raised the possibility of contamination.

References

Allen, M., Jackson, J., Walker, R., 2004. Late Cenozoic reorganization of the Arabia–Eurasia collision and the comparison of short-term and long-term deformation rates. Tectonics 23, TC2008. doi:10.1029/2003TC001530.

Almogi-Labin, A., Luz, B., Duplessy, J.-C., 1986. Quaternary paleoceanography, pteropod preservation and stable-isotope record of the Red Sea. Palaeogeography, Palaeoeclimatology, Palaeoecology 57, 195–211.

Almogi-Labin, A., Hemleben, C., Meischner, D., Erlenkeuser, H., 1991. Paleoenvironmental events during the last 13,000 years in the central Red Sea as recorded by pteropoda. Paleoceanography 6, 83–98.

Ambraseys, N.N., 2001. Reassessment of earthquakes, 1900–1999, in the Eastern Mediterranean and the Middle East. Geophysical Journal International 145, 471–485.

Anschutz, P., Blanc, G., Stille, P., 1995. Origin of fluids and the evolution of the Atlantis II deep hydrothermal system, Red Sea: strontium isotope study. Geochimica Cosmochimica Acta 59, 4799–4808.

Auras-Schudnagies, A., Kroon, D., Ganssen, G., Hemleben, C., Van Hinte, J.E., 1989. Distributional pattern of planktonic foraminifers and pteropods in surface waters and top core sediments of the Red Sea, and adjacent areas controlled by the monsoonal regime and other ecological factors. Deep-Sea Research 36, 1515–1533.

Bach, W., Humphris, S.E., 1999. Relationship between the Sr and O isotope compositions of hydrothermal fluids and the spreading and magma-supply rates of oceanic spreading centers. Geology 27, 1067–1070.

Barberi, F., Ferrara, G., Santacroce, R., Varet, J., 1975. Structural evolution of the Afar Triple Junction. In: Pilger, A., Rosler, A. (Eds.), Afar Depression of Ethiopia. Schweitzerbart, Stuttgart, pp. 38–54.

Ben-Menahem, A., 1991. Four thousand years of seismicity along the Dead Sea Rift. Journal of Geophysical Research 96, 20195–20216.

Berggren, W.A., 1969. Micropaleontologic investigations of Red Sea cores—summation and synthesis of results. In: Degens, E.T., Ross, D.A. (Eds.), Hot Brines and Recent Heavy Metal Deposits in the Red Sea. Springer-Verlag, New York, pp. 329–335.

Blanc, G., Boulègue, J., Michard, A., 1995. Isotope C3 stage Red Sea floor spreading. Nature 247, 7–11.

Boger, P.D., Faure, G., 1974. Strontium-isotope stratigraphy of a Red Sea core. Geology 2, 81–83.

Boger, P.D., Faure, G., 1976. Systematic variations of sialic and volcanic detritus in piston cores from the Red Sea. Geochimica Cosmochimica Acta 40, 731–742.

Boger, P.D., Boger, J.L., Faure, G., 1980. Systematic variations of $^{87}Sr/^{86}Sr$ ratios, Sr compositions, selected major-oxide concentrations, and mineral abundances in piston cores from the Red Sea. Chemical Geology 29, 13–38.

Bonatti, E., 1985. Punctiform initiation of seafloor-spreading in the Red Sea. Nature 316, 33–37.

Bosworth, W., Taviani, M., 1996. Late Quaternary reorientation of stress field and extension direction in the southern Gulf of Suez, Egypt: evidence from uplifted coral terraces, mesoscopic fault arrays, and borehole breakouts. Tectonics 15, 791–802.

Brewer, P.G., Riley, J.P., Culkin, F., 1965. The chemical composition of the hot salty water from the bottom of the Red Sea. Deep-Sea Research 12, 497–503.

Chu, D., Gordon, R.G., 1998. Current plate motions across the Red Sea. Geophysical Journal International 135, 313–328.

Cocherie, A., Calvez, J.Y., Oudin-Dunlop, E., 1994. Hydrothermal activity as recorded by Red Sea sediments: Sr–Nd isotopes and REE signatures. Marine Geology 118, 291–302.

Deuser, W.G., Degens, E.T., 1969. O^{18}/O^{16} and C^{13}/C^{12} ratios of fossils from the hot-brine deep area of the central Red Sea. In: Degens, E.T., Ross, D.A. (Eds.), Hot Brines and Recent Heavy Metal Deposits in the Red Sea. Springer-Verlag, New York, pp. 336–347.

Ehrlich, S., Gavrieli, I., Ben Dor, L., Halicz, L., 2001. Direct high precision measurements of the $^{87}Sr/^{86}Sr$ isotope ratio in natural water, carbonates and related materials by multiple collector inductively coupled plasma mass spectrometry (MC-ICP-MS). Journal of Analytical Atomic Spectroscopy 16, 1389–1392.

Faure, G., 1986. Principles of Isotope Geology, 2nd ed Wiley, New York.

Girdler, R.W., Styles, P., 1974. Two stage Red Sea floor spreading. Nature 247, 7–11.

Hartmann, M., Scholten, J.C., Stoffers, P., 1998. Hydrographic structure of brine-filled deeps in the Red Sea: correction of Atlantis II Deep temperatures. Marine Geology 144, 331–332.

Hibsch, C., Jarrige, J.-J., Cushing, E.M., Mercier, J., 1995. Palaeostress analysis, a contribution to the understanding of basin tectonics and geodynamic evolution. Example of the Permian/Cenozoic tectonics of Great Britain and geodynamic implications in western Europe. Tectonophysics 252, 103–136.

Johnson, H.P., Dziak, R.P., Fisher, C.R., Fox C.G., Pruis, M.J., 2001. Earthquakes' impact on hydrothermal systems may be far-reaching. EOS Transactions of the American Geophysical Union 82, 233, 236.

Ken-Tor, R., Agnon, A., Enzel, Y., Stein, M., Marco, S., Negendank, J.F.W., 2001. High-resolution geological record of historic earthquakes in the Dead Sea basin. Journal of Geophysical Research 106, 2221–2234.

Ku, T.L., Thurber, D.L., Mathieu, G.G., 1969. Radiocarbon chronology of the Red Sea sediments. In: Degens, E.T., Ross, D.A. (Eds.), Hot Brines and Recent Heavy Metal Deposits in the Red Sea. Springer-Verlag, New York, pp. 348–359.

McClusky, S., Reilinger, R., Mahmoud, S., Ben Sari, D., Tealeb, A., 2003. GPS constraints on Africa (Nubia) and Arabia plate motions. Geophysical Journal International 155, 126–138.

Makris, J., Franke, M., Grützner, J., 1991. Microearthquake activity in the Suakin deep, Red Sea, and tectonic implications. Tectonophysics 198, 411–420.

Marco, S., Stein, M., Agnon, A., Ron, H., 1996. Long-term earthquake clustering: a 50,000-year paleoseismic record in the Dead Sea Graben. Journal of Geophysical Research 101, 6179–6191.

Milliman, J.D., Ross, D.A., Ku, T.-L., 1969. Precipitation and lithification of deep-sea carbonates in the Red Sea. Journal of Sedimentary Petrology 39, 724–736.

Muehlenbachs, K., Clayton, R.N., 1976. Oxygen isotope composition of oceanic crust and its bearing on seawater. Journal of Geophysical Research 81, 4365–4369.

Naqvi, W.A., Fairbanks, R.G., 1996. A 27,000 year record of Red Sea outflow: implication for timing of post-glacial monsoon intensification. Geophysical Research Letters 23, 1501–1504.

Omar, G.I., Steckler, M.S., 1995. Fission track evidence on the initial rifting of the Red Sea: two pulses, no propagation. Science 270, 1341–1344.

Pierret, M.C., Clauer, N., Bosch, D., Blanc, G., France-Lanord, C., 2001. Chemical and isotopic ($^{87}Sr/^{86}Sr$, $\delta^{18}O$, δD) constraints to the formation processes of Red-Sea brines. Geochimica Cosmochimica Acta 65, 1259–1275.

Plenefisch, T., Bonjer, K.-P., 1997. The stress field in the Rhine Graben area inferred from earthquake focal mechanisms and estimation of frictional parameters. Tectonophysics 275, 71–97.

Sanchez Almazo, I., Spiro, B., Braga, J.C., Martin, J.M., 2001. Constraints of stable isotope signatures on the depositional palaeoenvironments of upper Miocene reef and temperate carbonates in the Sorbas basin, SE Spain. Palaeogeography, Palaeoclimatology and Palaeoecology 175, 153–172.

Schoell, M., Risch, H., 1976. Oxygen- and carbon-isotope analyses on planktonic Foraminifera of Core VA 01-188P (southern Red Sea). Geologische Jahrbuch 17, 15–32.

Scholten, J.C., Stoffers, P., Walter, P., Plüger, W., 1991. Evidence for episodic hydrothermal activity in the Red Sea from the composition and formation of hydrothermal sediments, Thetis Deep. Tectonophysics 190, 109–117.

Shackleton, N.J., Berger, A., Peltier, W.R., 1990. An alternative astronomical calibration of the Lower Pleistocene timescale based on ODP site 677. Royal Society of Edinburgh, Earth Sciences, Transactions 81, 251–261.

Shamir, G., Baer, G., Hofstetter, A., 1993. Three-dimensional elastic earthquake modelling based on integrated seismological and InSAR data: the $M_w = 7.2$ Nuweiba earthquake, gulf of Elat/Aqaba 1995 November. Geophysical Journal International 154, 731–744.

Siddall, M., Rohling, E.J., Almogi-Labin, A., Hemleben, Ch., Meischner, D., Schmelzer, I., Smeed, D.A., 2003. Sea-level fluctuations during the last glacial cycle. Nature 423, 853–858.

Siddall, M., Smeed, D.A., Hemleben, C., Rohling, E.J., Scmelzer, I., Peltier, W.R., 2004. Understanding the Red Sea response to sea level. Earth and Planetary Science Letters 225, 421–434.

Spooner, E.T.C., Chapman, H.J., Smewing, J.D., 1977. Strontium isotopic contamination and oxidation during ocean floor hydrothermal metamorphism of the ophiolitic rocks of the Troodos Complex, Cyprus. Geochimica Cosmochimica Acta 41, 873–890.

Starinsky, A., Stein, M., Almogi-Labin, A., Goldstein, S.L., Hemleben, C., 2002. Strontium isotopes in the Red Sea–Gulf of Aden during the past 530 kyr: the role of hydrothermal and "erosional" components during glacial interglacial cycles. Geochimica Cosmochimica Acta 66, A735.

Ten Veen, J.H., Postma, G., 1999. Neogene tectonics and basin fill patterns in the Hellenic outer-arc (Crete, Greece). Basin Research 11, 223–241.

Thunell, R.C., Locke, S.M., Williams, D.F., 1988. Glacio-eustatic sea-level controls on Red Sea salinity. Nature 334, 601–604.

Vance, D., Scrivner, A.E., Beney, P., Staubwasser, M., Henderson, G.M., Slowey, N.C., 2004. The use of foraminifera as a record of past neodymium isotope composition of seawater. Palaeogeography 19, Art. No. PA 2009.

Vernant, Ph., et al., 2004. Present-day crustal deformation and plate kinematics in the Middle East constrained by GPS measurements in Iran and northern Oman. Geophysical Journal International 157, 381–398.

Vita-Finzi, C., 2001. Neotectonics at the Arabian plate margins. Journal of Structural Geology 23, 521–530.

Wernicke, B., Friedrich, A.M., Niemi, N.A., Bennett, R.A., Davis, J.L., 2000. Dynamics of plate boundary fault systems from Basin and Range geodetic network (BARGEN) and geologic data. GSA Today 10, 1–2.

Zain Eldeen, U., Delvaux, D., Jacobs, P., 2002. Tectonic evolution in the Wadi Araba Segment of the Dead Sea Rift, South-West Jordan. In: Cloetingh, S.A.P.L., Ben-Avraham, Z. (Eds.), From Continental Extension to Collision: Africa–Europe Interaction, the Dead Sea and Analogue Natural Laboratories. Stephan Mueller Special Publication Series 2, pp. 63–81.